Evidence for Electron Capture of an Outgoing Photoelectron Wave by a Non-valence State in $(C_6F_6)_n^-$

*Joshua P. Rogers, Cate S. Anstöter, and Jan R. R. Verlet**

Department of Chemistry, Durham University, Durham DH1 3LE, United Kingdom.

*Corresponding author: j.r.r.verlet@durham.ac.uk

ABSTRACT

Frequency-resolved photoelectron spectra are presented for $(C_6F_6)_n^-$ with n = 1-5 that show that $C_6F_6^-$ is solvated by neutral C_6F_6 molecules. Direct photo-detachment channels of $C_6F_6^-$ are observed for all n, leaving the neutral in the S_0 ground state or triplet states, T_1 and T_2. For $n \geq 2$, an additional indirect electron loss channel is observed when the triplet state channels open. This indirect emission appears to arise from the electron capture of the outgoing photoelectron s-wave by a neutral solvent molecule through an anion non-valence state. The same process is not observed for the S_0 detachment channel because the outgoing electron wave is predominantly a p-wave. Our results show that anion non-valence states can act as electron accepting states in cluster environments and can be viewed as precursor states for diffuse states of liquid C_6F_6.

TOC GRAPHICS

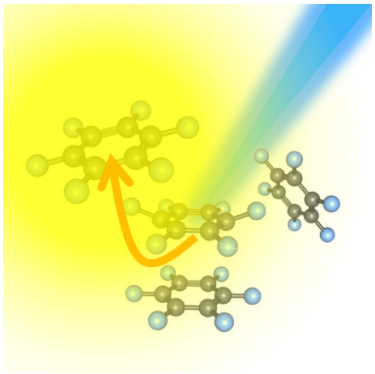

Non-valence states of anions have been invoked as doorway states for low energy electron attachment to molecules and can be viewed as precursors for charge-transfer states in the bulk and as molecular analogues of a conduction band. In contrast to the well-known neutral case of Rydberg states, non-valence states in anions are not bound by the Coulomb potential. Instead, electrostatic potentials, such as the permanent dipole of a neutral core, can lead to electron binding if the dipole moment exceeds a critical value of ~2.5 D.[1,2] Similar to these so-called dipole-bound states, quadrupole-electron interactions (or higher multipoles) can also lead to binding to form quadrupole-bound states.[3–5] Beyond these electrostatic interactions, correlation forces can also bind electrons, leading to so-called non-valence correlation-bound states.[6–13] In reality, it is often a combination of these interactions that bind the electron in a very diffuse non-valence orbital.[2] The binding energy of such an orbital is typically very small, less than a few 100 meV. It is their energetic proximity to the neutral threshold and their large spatial distribution that make non-valence orbitals excellent accepting states for incoming low-energy electrons.[10,14,15] A classic example of low-energy attachment is hexafluorobenzene, C_6F_6. Field *et al*. observed a large increase in cross section very close to threshold for s-wave electron scattering,[16] which could arise from the presence of a non-valence correlation-bound state that was predicted by Voora and Jordan.[10] This non-valence state adiabatically connects to the valence ground state of $C_6F_6^-$ and the mechanism of this slow-electron attachment process was recently probed in real-time using iodide as a source of electrons in the $I^-(C_6F_6)$ system.[14]

The specific interest in C_6F_6 electron attachment is in part motivated by the observation that in bulk liquid C_6F_6, the electron mobility was measured to be anomalously high and could not be assigned to the diffusion of the valence-bound $C_6F_6^-$ solute in a C_6F_6 solvent.[17] It is instead believed that delocalised electron states may be responsible for the high electron

mobility.[17] Diffuse states have also been invoked to explain observations in two-photon emission spectroscopy of cold C_6F_6 monolayers deposited on a Cu(111) surface in ultrahigh vacuum.[18,19] It is thought that these delocalized states are related on a molecular level to the non-valence correlation-bound state of $C_6F_6^-$.[10]

To gain additional insight into the electronic states and electron injection into C_6F_6 and to attempt to bridge the gap between the single molecule and condensed phase observations, we present a frequency-resolved (2D) photoelectron (PE) imaging study[20–22] of anionic hexafluorobenzene clusters, $(C_6F_6)_n^-$ with n = 1-5. The PE spectra show evidence of s-wave electron capture of the outgoing electron wave, while for an outgoing p-wave, such capture is not seen. Our observations are consistent with electron capture by a non-valence correlation-bound state,[14,16] enabled by the presence of the solvent.

Figure 1 shows the 2D-PE spectra of $(C_6F_6)_n^-$ for n = 1-5 taken over a photon energy range $1.8 \leq h\nu \leq 5.8$ eV. The individual PE spectra are given in the Supporting Information and each PE spectrum in Figure 1 has been normalized to its total integrated intensity. For n = 1 and 2, the PE are acquired at every $h\nu$ = 0.1 eV interval, while for $n \geq 3$, we had to increase this interval to 0.5 eV because of the reduced signal levels for the larger clusters. Starting with n = 1, in Figure 1(a) several features are identified. Features (i), (ii) and (iii) increase in electron kinetic energy (eKE) by an amount equal to the increase in $h\nu$ and can be identified as direct detachment channels. For brevity, only features pertinent to the current work will be given here and a detailed analysis will be provided elsewhere. Feature (i) at highest eKE corresponds to the $D_0 + h\nu \rightarrow S_0 + e^-$ direct detachment channel, where S_0 represents the neutral ground state (singlet) and D_0 is the radical electronic ground state of $C_6F_6^-$. Features (ii) and (iii), appearing around 3.9 and 4.9 eV, correspond to the $D_0 + h\nu \rightarrow T_1 + e^-$ and the $D_0 + h\nu \rightarrow T_2 + e^-$ direct detachment

channels, respectively, where T_1 and T_2 are the first and second excited triplet states of the neutral C_6F_6. For $h\nu > 5.0$ eV, the apparent disappearance of channels (i) and (ii) is an artefact of the normalization: the $D_0 + h\nu \rightarrow T_2 + e^-$ direct detachment channels has a much larger cross section than the $D_0 + h\nu \rightarrow S_0 + e^-$ and $D_0 + h\nu \rightarrow T_1 + e^-$ channels (individual PE spectra are given in the Supporting Information).

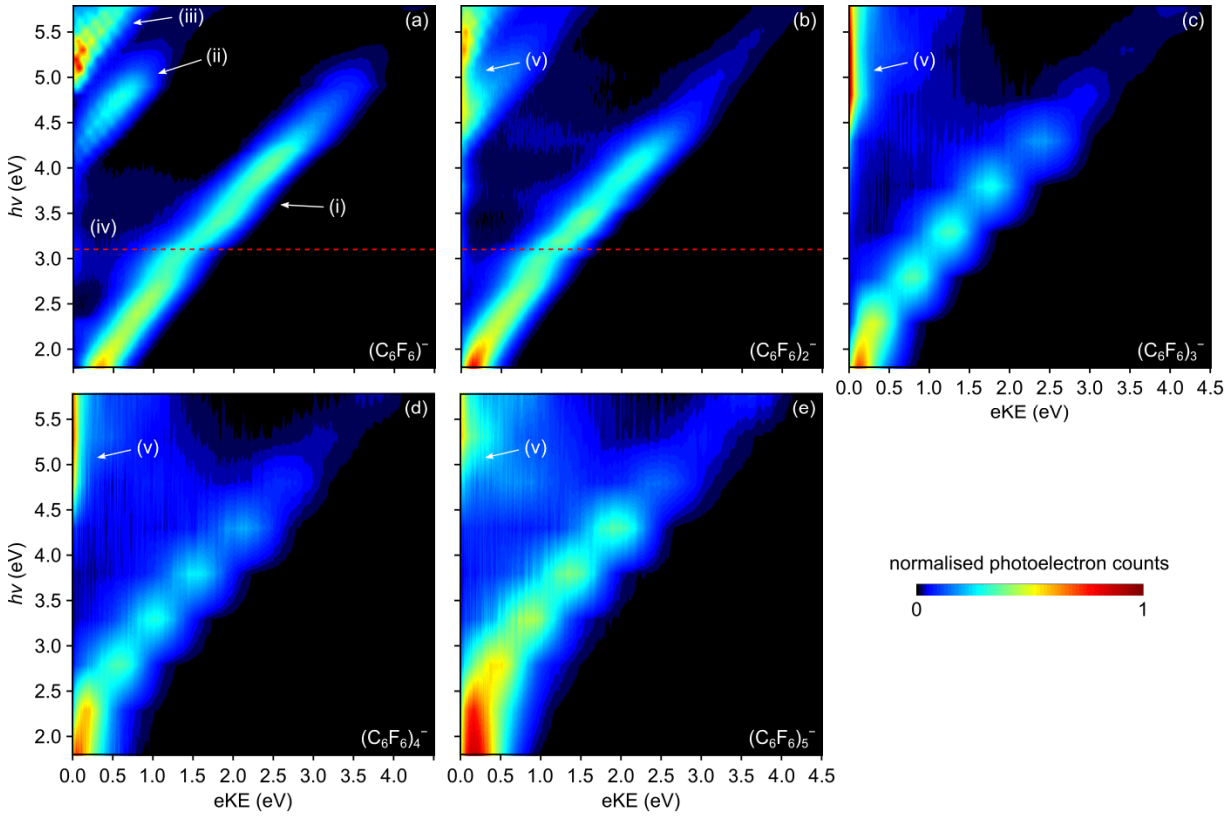

Figure 1. 2D Photoelectron spectra of $(C_6F_6)_n^-$ with n = 1 to 5 in (a) to (e). Features (i), (ii) and (iii) correspond to direct detachment of $C_6F_6^-$ leaving the neutral in the S_0, T_1, or T_2 electronic states, respectively. Feature (iv) arises from delayed autodetachment resonances excited in $C_6F_6^-$. Feature (v) arises from an indirect mechanism associated with the formation of a non-valence state (see text) and is only seen for $n \geq 2$. The red dashed line indicates where the light source changes its output and is very weak.

The spectral width of the $D_0 + h\nu \rightarrow S_0 + e^-$ channel is consistent with previous PE spectroscopy studies by the Kaya[23] and Bowen[26] groups and arises from the large structural change upon photodetachment from the buckled D_0 valence ground state of $C_6F_6^-$ (C_{2v} symmetry) to the planar S_0 ground state of neutral C_6F_6 (D_{6h} symmetry). Both the T_1 and T_2 states of the neutral have buckled geometries that are more similar to that of the D_0 anion state and vibrational structure can be seen in the PE features (ii) and (iii) (see Supporting Information). The non-valence state of $C_6F_6^-$ has the nuclear geometry of that of the S_0 state owing to the very weak interaction of the diffuse orbital with the neutral core.[10,14] While there are clear signatures of dynamics involving resonances in the 2D-PE spectra (feature (iv) in Figure 1(a)),[22,24–26] there is no apparent evidence for the formation of the non-valence state of $C_6F_6^-$.[14] This is of course not surprising given that the Franck-Condon overlap between anion and the neutral ground states is poor.[23,27]

Figure 1(b) to (e) show the 2D-PE spectra for $(C_6F_6)_n^-$ with n = 2 to 5, respectively. For n = 3 to 5, we have taken fewer PE spectra because of their reduced abundance in the molecular beam. Nevertheless, we have also plotted these as false-colour plots, which includes a linear interpolation along the $h\nu$ axis to emphasize changes as a function of $h\nu$ and to assist comparison between different n. We note that this interpolation leads to the apparent oscillations in the 2D-PE spectra which are a consequence of under-sampling (i.e. PE spectra taken at $h\nu$ = 0.5 eV intervals for $n \geq 3$), but it does not affect the final conclusions.

Comparison of Figure 1(a) with Figures 1(b) to (e) shows the same overall features. The $D_0 + h\nu \rightarrow S_0 + e^-$ direct detachment channel can be identified for all clusters studied and the corresponding PE spectra have a very similar distribution. Hence, the clusters can be viewed as being composed of the buckled D_0 valence ground state of $C_6F_6^-$ solvated by neutral C_6F_6

molecules, $C_6F_6^-(C_6F_6)_{n-1}$. The increase in vertical detachment energy (~200n meV) with increasing n arises from to the incremental cohesion energy of the solvent C_6F_6 molecules to the $C_6F_6^-$ solute anion, and is consistent with the previous study by the Kaya and coworkers.[23] As expected, the $D_0 + h\nu \rightarrow T_1 + e^-$ and the $D_0 + h\nu \rightarrow T_2 + e^-$ direct detachment channels are also observed for all n in Figure 1 (although the data for $n = 5$ is of poorer quality). Overall, while there are some differences in the location and dynamics of the observed resonances, the 2D-PE spectroscopy of the different clusters is very similar.

Despite the similarity, one key difference between $n = 1$ and $n \geq 2$ is that the apparent opening of the $D_0 + h\nu \rightarrow T_1 + e^-$ and the $D_0 + h\nu \rightarrow T_2 + e^-$ detachment channels leads to the production of slow electrons, as evidenced by the peak at eKE ~ 0 eV indicated by (v) in Figures 1(b) to (e). The onset of these slow electrons appears to increase with n in a similar manner as the increase in vertical detachment energy, however, the relatively sparse sampling precludes a quantitative analysis. The observation of low energy electrons is counter-intuitive because the opening of a direct detachment channel is associated with instant electron emission (i.e. vertical Franck-Condon profile) while the slow electrons are indicative of an indirect electron loss channel.[28–33] The observation that the slow electrons are only present for $n \geq 2$ suggests that their origin is related to the cluster environment. However, we will first consider the detachment from isolated $C_6F_6^-$ in more detail.

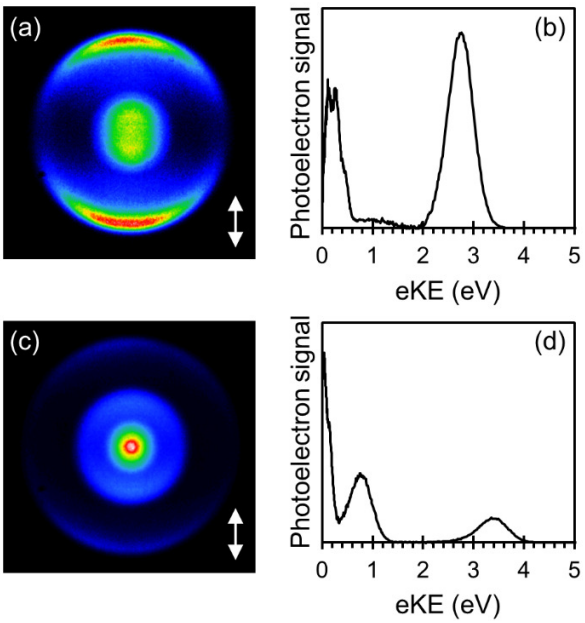

Figure 2. A raw photoelectron image (a) and spectrum (b) of $C_6F_6^-$ taken at $h\nu$ = 4.3 eV, and at $h\nu$ = 5.0 eV in (c) and (d), respectively. The images indicate the representative photoelectron angular distribution of the different direct detachment channels. The polarization axis is indicated as the double arrow.

Figure 2(a) and (c) shows a raw PE image of $C_6F_6^-$ taken at $h\nu$ = 4.3 and 5.0 eV along with the resulting PE spectrum in Figure 2(b) and (d), respectively. The feature with the largest radius in the PE image corresponds to the high eKE peak and shows that the $D_0 + h\nu \rightarrow S_0 + e^-$ process leads to a highly anisotropic PE angular distribution (PAD), peaking parallel to the polarization axis of the light. The PAD is sensitive to the orbital from which the electron is detached and defines the partial wave contributions to the outgoing electron.[34–37] For the buckled D_0 state of $C_6F_6^-$, predominant p-wave emission is expected because of the σ* character of the singly-occupied molecular orbital, which leads to the observed PAD.[34,36] This is in agreement

with our calculations for the PAD of the $D_0 + h\nu \rightarrow S_0 + e^-$ channel (see Supporting Information). The PE spectra in Figure 1(a) also support that the $D_0 + h\nu \rightarrow S_0 + e^-$ leads to p-wave emission. For $h\nu < 2.0$ eV, there is a distinct lack of PE emission at very low eKE. According to Winger's threshold law,[38] the emission cross-section, σ_l, scales as $eKE^{l+1/2}$. Hence, for $l = 0$, there is a rapid rise in σ_0 above the threshold, while for $l = 1$, a much slower rise in σ_1 is expected because of the centrifugal barrier. Thus, the PE signal should be rising slowly from eKE = 0 eV for p-wave emission, consistent with the observed spectral shape for $h\nu < 2.0$ eV.

In contrast to the strong anisotropic emission for the $D_0 + h\nu \rightarrow S_0 + e^-$ channel, Figure 2 shows that the $D_0 + h\nu \rightarrow T_1 + e^-$ and the $D_0 + h\nu \rightarrow T_2 + e^-$ photoemission channels are much less anisotropic. The departing PE contains large contributions from $l = 0$ partial waves, especially at low eKE because of the σ scaling. Again, the PE spectra are consistent with this interpretation and are also supported by our calculations that show the interplay between partial waves in the photoemission of the $D_0 + h\nu \rightarrow T_1/T_2 + e^-$ channels (see Supporting Information).

We now consider the effect of clustering. The PE images for the clusters show that the photoemission process from the solute $C_6F_6^-$ remains unchanged near threshold: p-wave emission dominates for the $D_0 + h\nu \rightarrow S_0 + e^-$ channel and s-wave emission dominates for the $D_0 + h\nu \rightarrow T_1/T_2 + e^-$ channels. But in the cluster, the outgoing waves encounter neutral solvent molecules. The neutral solvent molecules are close to planar so that they have the correct geometry to support a non-valence state of their anion.[10] According to Voora and Jordan, the electronic nature of the non-valence state is predominantly of s-character with a_{1g} symmetry.[10] To a first approximation, for the non-valence state to serve as a doorway state, the incoming electron must have the correct symmetry: an s-wave can be captured, while a p-wave cannot be captured by the non-valence state.[16] Hence, for the $D_0 + h\nu \rightarrow S_0 + e^-$ detachment channel, the

outgoing p-wave does not have the correct symmetry and therefore cannot be trapped by the solvent molecules' non-valence anion state. For the $D_0 + h\nu \rightarrow T_1/T_2 + e^-$ channels, the s-wave can be captured. The capture of the outgoing s-wave electron leads to a temporary negative ion that then undergoes statistical electron detachment, similar to the observations of low-energy electron attachment to neutral C_6F_6,[16,39] which produces a characteristic electron distribution peaking at 0 eV.[28] This electron capture mechanism, shown schematically in Figure 3, provides a consistent explanation of why slow electrons are observed only when the $D_0 + h\nu \rightarrow T_1/T_2 + e^-$ channels open; and not for the $D_0 + h\nu \rightarrow S_0 + e^-$ detachment channel; and only for clusters ($n \geq 2$). The slow electrons are therefore a signature of intra-cluster electron capture. We also note that the presence of the centrifugal barrier to p-wave detachment for the $D_0 + h\nu \rightarrow S_0 + e^-$ channel means that the emission of slow electrons with sufficiently low energy for capture by neutral solvent molecules would be inhibited. We note however that the above picture based on symmetry arguments assumes an isolated particle. This is not the case in the cluster environment and p-wave emission from $C_6F_6^-$ is likely to have an s-wave contribution on a neighboring C_6F_6 solvent molecule. A quantitative analysis of the extent of this contribution requires cluster structures, which are not available from the current experiments.

While the above mechanism is consistent with the observations, we briefly comment on other possible mechanisms leading to low energy electron emission. The most commonly observed source of slow electrons is thermionic emission,[28] which comes about from the statistical electron loss of the hot electronic ground state that was produced by internal conversion from initially excited valence resonances.[33,40] While we observe dynamics involving resonances, as evidenced by PE emission at lower eKE than the direct detachment channels (feature (iv) in Figure 1),[22] there is no clear indication that the ground state is efficiently

recovered and thermionic emission is not observed when fingerprints of resonances are seen in Figure 1. Moreover, it would be peculiar that the resonances would ultimately decay by thermionic emission only for $n \geq 2$ and not for $n = 1$. While resonances may decay differently in the monomer than in the cluster because the cluster environment can alter the resonance position and decay dynamics, it would be very coincidental that the appearance of the thermionic emission closely follows the opening of the $D_0 + h\nu \rightarrow T_1/T_2 + e^-$ channels. Finally, one might anticipate that resonances excited closer to the adiabatic threshold would be more likely to reform the ground state by internal conversion, which is not what is observed in Figure 1.

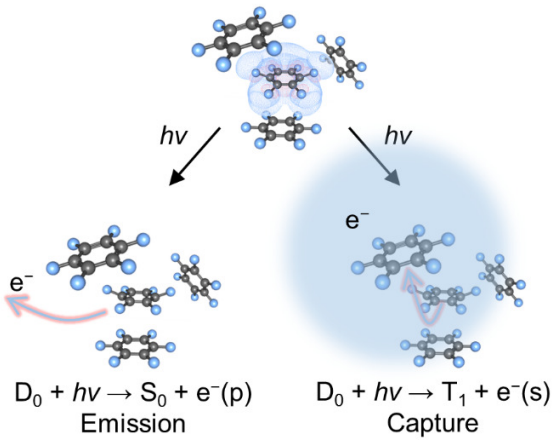

Figure 3. Schematic of electron capture mechanism that gives rise to the low-energy electrons observed in Figure 1. Photoemission from $C_6F_6^-$ in the cluster can lead to p-wave emission or s-wave emission, depending on the detachment channel. Only s-wave emission can lead to electron capture via a non-valence state of the cluster.

The mechanism depicted in Figure 3 appears to occur even with a single C_6F_6 solvent molecule (Figure 1(b)), although the relative PE signal at eKE ~ 0 eV is more intense for $n \geq 3$, suggesting a more efficient intra-cluster electron capture for these. While a single C_6F_6 can support a non-valence bound state, Voora and Jordan also showed that $(C_6F_6)_2$ can support a non-valence state in which the electron is delocalized over both molecules.[10] Their calculation considered the dimer to be bound side-by-side (coplanar) with an inter molecular distance of 8 Å (motivated by two-photon photoemission experiments of monolayer C_6F_6 on Cu(111) surfaces[19]), and although this is not likely to be the structure of the solvent in $(C_6F_6)_n^-$, their results show that co-operative effects can lead to binding, and that the non-valence state can delocalize throughout a very large volume.[10] In our cluster experiments, the non-valence state formed upon photoemission is likely associated with more than one solvent molecule, which may explain the increase in low energy electron signal for $n \geq 3$, where multiple solvent molecules can participate.

The dynamics of electron capture have recently been probed by time-resolved PE spectroscopy using photodetachment of I^- as a source of electrons.[14] This showed that the initially formed non-valence state evolves into the valence bound state of $C_6F_6^-$ within ~30 fs, followed by coherent motion of the buckling mode connecting the S_0 and D_0 geometries.[14] The fate and dynamics of a non-valence state involving more than one C_6F_6 are not known. For example, the non-valence state may collapse into a valence state of a single molecule or there may be a barrier preventing the rapid decay of the non-valence state. It is also interesting to note that the charge injection leaves the neutral from which photodetachment occurred in an excited state (T_1 or T_2) so that there is a large amount of excess energy in the system. While we can

observe the loss of slow electrons, our current measurements do not probe the dynamics of their formation.

Finally, we compare the present work with studies in para-toluquinone anionic clusters $(pTQ)_n^-$,[7,20] and the iodide-solvent clusters: $I^-(Xe)_n$ and $I^-(H_2O)_n$ clusters.[41–45] In $(pTQ)_n^-$, the electron is similarly localized on a single pTQ that is solvated by neutral pTQ molecules, similar to the $(C_6F_6)_n^-$ case. While $(pTQ)_2^-$ showed evidence for dissociation,[20] time-resolved PE spectroscopy of $(pTQ)_3^-$ also showed the formation of a non-valence state.[7] However, the dynamics in this cluster were interpreted in terms of an internal conversion from an initially photoexcited π^* resonance into a non-valence state of the cluster. The indirect electron loss channel also showed vibrational structure that was assigned to the vibrational autodetachment of the non-valence state by specific modes of the cluster. A similar mechanism was observed in a different quinone dimer anion.[46] In $(C_6F_6)_n^-$, no such structure was seen suggesting a more statistical (and probably slower) electron emission. The comparison to iodide:solvent clusters is also interesting. In those cases, a bright absorption band corresponds to the charge-transfer-to-solvent band.[41,43] Excitation to this band leads initially to a diffuse non-valence state associated with the entire cluster.[42,44] For $I^-(Xe)_n$, the non-valence state undergoes only decay dynamics with little solvation, presumably leading to the $(Xe)_n^-$ species observed by mass spectrometry.[47] For $I^-(H_2O)_n$ with $n > 10$, the initially excited non-valence state could be correlated with the surface-bound electron of a water cluster,[45,48] which was subsequently stabilized by rapid solvent rearrangement. These dynamics have also been observed at the ambient water/air interface[49] and suggest that the cluster environments indeed offer a useful molecular-level description of bulk phenomena. The dynamics proposed in $(C_6F_6)_n^-$ bear many resemblances to the iodide-solvent clusters including formation of a non-valence state and thermionic emission.

In summary, we have shown compelling evidence that photoemission from $(C_6F_6)_n^-$ can lead to electron capture by the solvent molecules that is mediated by a diffuse non-valence anion state. Our results provide additional evidence for the importance and probable ubiquity of non-valence anion states. These states manifest as precursors for bulk charge-transfer states and conduction bands, and the study of their existence and formation in clusters is likely to provide new molecular-level insights into bulk properties.

EXPERIMENTAL METHODS

Experimentally, C_6F_6 anions and anionic clusters were generated in a molecular beam source by seeding Ar carrier gas with the vapour pressure of liquid C_6F_6, expanding the mixture through a pulsed valve, and crossing the expansion with a 300 eV electron beam. Ions were mass-selected in a time-of-flight mass-spectrometer and intersected with light at the center of a perpendicular velocity-map PE imaging spectrometer.[50] The electric field strength in the interaction region was 250 V cm^{-1}, which is insufficient to detach an electron from a non-valence state bound by > 100 meV as is the case in $C_6F_6^-$.[10] Photodetachment was performed using tunable light from a Nd:YAG pumped OPO providing ~5 ns pulses and covering a wavelength range from 200 – 2500 nm. There is a change in optical alignment required at 400 nm (3.10 eV) and the pulse energy at this wavelength is very poor (indicated by red dashed line in Figure 1). PE images were analyzed using polar onion peeling[51] and the PE spectrometer was calibrated using the known PE spectrum of O_2^- and has a spectral resolution of $\Delta eKE/eKE < 3$ %.

ASSOCIATED CONTENT

Supporting Information. Individual photoelectron spectra that were used to prepare Figure 1; and photoelectron angular distributions for the three direct detachment channels. The following file (xlsx) is available free of charge: (C6F6)n_PE_spectra.xlsx

AUTHOR INFORMATION

The authors declare no competing financial interests. Corresponding author indicated by asterisk, j.r.r.verlet@durham.ac.uk.

ACKNOWLEDGMENT

This work was supported by the European Research Council through Starting Grant 306536.

REFERENCES

(1) Jordan, K. D.; Wang, F. Theory of Dipole-Bound Anions. *Annu. Rev. Phys. Chem.* **2003**, *54*, 367–396.

(2) Simons, J. Molecular Anions. *J. Phys. Chem. A* **2008**, *112*, 6401–6511.

(3) Sommerfeld, T.; Dreux, K. M.; Joshi, R. Excess Electrons Bound to Molecular Systems with a Vanishing Dipole but Large Molecular Quadrupole. *J. Phys. Chem. A* **2014**, *118*, 7320–7329.

(4) Zhu, G.-Z.; Liu, Y.; Wang, L.-S. Observation of Excited Quadrupole-Bound States in Cold Anions. *Phys. Rev. Lett.* **2017**, *119*, 023002.

(5) Garrett, W. R. Quadrupole-Bound Anions: Efficacy of Positive versus Negative Quadrupole Moments. *J. Chem. Phys.* **2012**, *136*, 054116.

(6) Bezchastnov, V. G.; Vysotskiy, V. P.; Cederbaum, L. S. Anions of Xenon Clusters Bound by Long-Range Electron Correlations. *Phys. Rev. Lett.* **2011**, *107*, 133401.

(7) Bull, J. N.; Verlet, J. R. R. Observation and Ultrafast Dynamics of a Nonvalence Correlation-Bound State of an Anion. *Sci. Adv.* **2017**, *3*, e1603106.

(8) Klaiman, S.; Gromov, E. V.; Cederbaum, L. S. Extreme Correlation Effects in the Elusive Bound Spectrum of C_{60}^-. *J. Phys. Chem. Lett.* **2013**, *4*, 3319–3324.

(9) Sommerfeld, T.; Bhattarai, B.; Vysotskiy, V. P.; Cederbaum, L. S. Correlation-Bound Anions of NaCl Clusters. *J. Chem. Phys.* **2010**, *133*, 114301.

(10) Voora, V. K.; Jordan, K. D. Nonvalence Correlation-Bound Anion State of C_6F_6: Doorway to Low-Energy Electron Capture. *J. Phys. Chem. A* **2014**, *118*, 7201–7205.

(11) Voora, V. K.; Cederbaum, L. S.; Jordan, K. D. Existence of a Correlation Bound S-Type Anion State of C_{60}. *J. Phys. Chem. Lett.* **2013**, *4*, 849–853.

(12) Voora, V. K.; Jordan, K. D. Nonvalence Correlation-Bound Anion States of Polycyclic Aromatic Hydrocarbons. *J. Phys. Chem. Lett.* **2015**, *6*, 3994–3997.

(13) Sommerfeld, T. Excess Electrons Bound to Small Ammonia Clusters. *J. Phys. Chem. A* **2008**, *112*, 11817–11823.

(14) Rogers, J. P.; Anstöter, C. S.; Verlet, J. R. R. Ultrafast Dynamics of Low-Energy Electron Attachment via a Non-Valence Correlation-Bound State. *Nat. Chem.* **2018**, *10*, 341–346.

(15) Sommerfeld, T. Dipole-Bound States as Doorways in (Dissociative) Electron Attachment. *J. Phys. Conf. Ser.* **2005**, *4*, 245.

(16) Field, D.; Jones, N. C.; Ziesel, J.-P. Cold Electron Scattering in SF_6 and C_6F_6: Bound and Virtual State Channels. *Phys. Rev. A* **2004**, *69*, 052716.

(17) Nyikos, L.; Van den Ende, C. A. M.; Warman, J. M.; Hummel, A. High Mobility Excess Electrons in the Electron-Attaching Liquid Hexafluorobenzene. *J. Phys. Chem.* **1980**, *84*, 1154–1155.

(18) Dougherty, D. B.; Feng, M.; Petek, H.; Yates, J. T.; Zhao, J. Band Formation in a Molecular Quantum Well via 2D Superatom Orbital Interactions. *Phys. Rev. Lett.* **2012**, *109*, 266802.

(19) Gahl, C.; Ishioka, K.; Zhong, Q.; Hotzel, A.; Wolf, M. Structure and Dynamics of Excited Electronic States at the Adsorbate/Metal Interface: C_6F_6/Cu(111). *Faraday Discuss.* **2000**, *117*, 191–202.

(20) Bull, J. N.; Verlet, J. R. R. Dynamics of π*-Resonances in Anionic Clusters of Para-Toluquinone. *Phys. Chem. Chem. Phys.* **2017**, *19*, 26589–26595.

(21) West, C. W.; Bull, J. N.; Antonkov, E.; Verlet, J. R. R. Anion Resonances of Para-Benzoquinone Probed by Frequency-Resolved Photoelectron Imaging. *J. Phys. Chem. A* **2014**, *118*, 11346–11354.

(22) Anstöter, C. S.; Bull, J. N.; Verlet, J. R. R. Ultrafast Dynamics of Temporary Anions Probed through the Prism of Photodetachment. *Int. Rev. Phys. Chem.* **2016**, *35*, 509–538.

(23) Nakajima, A.; Taguwa, T.; Hoshino, K.; Sugioka, T.; Naganuma, T.; Oho, F.; Watanabe, K.; Nakao, K.; Konishi, Y.; Kishi, R.; et al. Photoelectron Spectroscopy of $(C_6F_6)^-_n$ and $(Au\text{-}C_6F_6)^-$ Clusters. *Chem. Phys. Lett.* **1993**, *214*, 22–26.

(24) Stanley, L. H.; Anstöter, C. S.; Verlet, J. R. R. Resonances of the Anthracenyl Anion Probed by Frequency-Resolved Photoelectron Imaging of Collision-Induced Dissociated Anthracene Carboxylic Acid. *Chem. Sci.* **2017**, *8*, 3054–3061.

(25) Anstöter, C. S.; Dean, C. R.; Verlet, J. R. R. Chromophores of Chromophores: A Bottom-up Hückel Picture of the Excited States of Photoactive Proteins. *Phys. Chem. Chem. Phys.* **2017**, *19*, 29772–29779.

(26) West, C. W.; Bull, J. N.; Hudson, A. S.; Cobb, S. L.; Verlet, J. R. R. Excited State Dynamics of the Isolated Green Fluorescent Protein Chromophore Anion Following UV Excitation. *J. Phys. Chem. B* **2015**, *119*, 3982–3987.

(27) Eustis, S. N.; Wang, D.; Bowen, K. H.; Naresh Patwari, G. Photoelectron Spectroscopy of Hydrated Hexafluorobenzene Anions. *J. Chem. Phys.* **2007**, *127*, 114312.

(28) Campbell, E. E. B.; Levine, R. D. Delayed Ionization and Fragmentation En Route to Thermionic Emission: Statistics and Dynamics. *Annu. Rev. Phys. Chem.* **2000**, *51*, 65–98.

(29) Campbell, E. E. B.; Ulmer, G.; Hertel, I. V. Delayed Ionization of C_{60} and C_{70}. *Phys. Rev. Lett.* **1991**, *67*, 1986–1988.

(30) Climen, B.; Pagliarulo, F.; Ollagnier, A.; Baguenard, B.; Concina, B.; Lebeault, M. A.; Lépine, F.; Bordas, C. Threshold Laws in Delayed Emission: An Experimental Approach. *Eur. Phys. J. D* **2007**, *43*, 85–89.

(31) Amrein, A.; Simpson, R.; Hackett, P. Multiphoton Excitation, Ionization, and Dissociation Decay Dynamics of Small Clusters of Niobium, Tantalum, and Tungsten: Time-resolved Thermionic Emission. *J. Chem. Phys.* **1991**, *95*, 1781–1800.

(32) Amrein, A.; Simpson, R.; Hackett, P. Delayed Ionization Following Photoexcitation of Small Clusters of Refractory Elements: Nanofilaments. *J. Chem. Phys.* **1991**, *94*, 4663–4664.

(33) Bull, J. N.; West, C. W.; Verlet, J. R. R. On the Formation of Anions: Frequency-, Angle-, and Time-Resolved Photoelectron Imaging of the Menadione Radical Anion. *Chem. Sci.* **2015**, *6*, 1578–1589.

(34) Reid, K. L. Photoelectron Angular Distributions. *Annu. Rev. Phys. Chem.* **2003**, *54*, 397–424.

(35) Cooper, J.; Zare, R. N. Angular Distribution of Photoelectrons. *J. Chem. Phys.* **1968**, *48*, 942–943.

(36) Sanov, A. Laboratory-Frame Photoelectron Angular Distributions in Anion Photodetachment: Insight into Electronic Structure and Intermolecular Interactions. *Annu. Rev. Phys. Chem.* **2014**, *65*, 341–363.

(37) Anstöter, C. S.; Dean, C. R.; Verlet, J. R. R. Sensitivity of Photoelectron Angular Distributions to Molecular Conformations of Anions. *J. Phys. Chem. Lett.* **2017**, *8*, 2268–2273.

(38) Wigner, E. P. On the Behavior of Cross Sections Near Thresholds. *Phys. Rev.* **1948**, *73*, 1002–1009.

(39) Suess, L.; Parthasarathy, R.; Dunning, F. B. Nondissociative Low-Energy Electron Attachment to SF_6, C_6F_6, $C_{10}F_8$, and c-C_7F_{14}: Negative Ion Lifetimes. *J. Chem. Phys.* **2002**, *117*, 11222–11227.

(40) Horke, D. A.; Li, Q.; Blancafort, L.; Verlet, J. R. R. Ultrafast Above-Threshold Dynamics of the Radical Anion of a Prototypical Quinone Electron-Acceptor. *Nat. Chem.* **2013**, *5*, 711–717.

(41) Becker, I.; Markovich, G.; Cheshnovsky, O. Bound Delocalized Excited States in $I^-(Xe)_n$ Clusters. *Phys. Rev. Lett.* **1997**, *79*, 3391–3394.

(42) Zanni, M. T.; Frischkorn, C.; Davis, A. V.; Neumark, D. M. Dynamics of the Charge-Transfer-to-Solvent States in $I^-(Xe)_n$ Clusters. *J. Phys. Chem. A* **2000**, *104*, 2527–2530.

(43) Serxner, D.; Dessent, C. E. H.; Johnson, M. A. Precursor of the I_{aq}^- Charge-transfer-to-solvent (CTTS) Band in $I^-(H_2O)_n$ Clusters. *J. Chem. Phys.* **1996**, *105*, 7231–7234.

(44) Lehr, L.; Zanni, M. T.; Frischkorn, C.; Weinkauf, R.; Neumark, D. M. Electron Solvation in Finite Systems: Femtosecond Dynamics of Iodide·(Water)$_n$ Anion Clusters. *Science* **1999**, *284*, 635–638.

(45) Verlet, J. R. R.; Kammrath, A.; Griffin, G. B.; Neumark, D. M. Electron Solvation in Water Clusters Following Charge Transfer from Iodide. *J. Chem. Phys.* **2005**, *123*, 231102.

(46) Bull, J. N.; West, C. W.; Verlet, J. R. R. Ultrafast Dynamics of Formation and Autodetachment of a Dipole-Bound State in an Open-Shell π-Stacked Dimer Anion. *Chem. Sci.* **2016**, *7*, 5352–5361.

(47) Haberland, H.; Kolar, T.; Reiners, T. Negatively Charged Xenon Atoms and Clusters. *Phys. Rev. Lett.* **1989**, *63*, 1219–1222.

(48) Verlet, J. R. R.; Bragg, A. E.; Kammrath, A.; Cheshnovsky, O.; Neumark, D. M. Observation of Large Water-Cluster Anions with Surface-Bound Excess Electrons. *Science* **2005**, *307*, 93–96.

(49) Nowakowski, P. J.; Woods, D. A.; Verlet, J. R. R. Charge Transfer to Solvent Dynamics at the Ambient Water/Air Interface. *J. Phys. Chem. Lett.* **2016**, *7*, 4079–4085.

(50) Lecointre, J.; Roberts, G. M.; Horke, D. A.; Verlet, J. R. R. Ultrafast Relaxation Dynamics Observed Through Time-Resolved Photoelectron Angular Distributions. *J. Phys. Chem. A* **2010**, *114*, 11216–11224.

(51) Roberts, G. M.; Nixon, J. L.; Lecointre, J.; Wrede, E.; Verlet, J. R. R. Toward Real-Time Charged-Particle Image Reconstruction Using Polar Onion-Peeling. *Rev. Sci. Instrum.* **2009**, *80*, 053104.